

# Oxidation of Bismuth Tellurite, $\text{Bi}_2\text{TeO}_5$

## I. Thermoanalytical and Optical Microscopic Studies

László Pöpl,<sup>\*,1</sup> István Földvári,<sup>†</sup> and Gábor Várhegyi<sup>‡</sup>

<sup>\*</sup>Institute of Inorganic and Analytical Chemistry, Loránd Eötvös University, P.O. Box 32, 1518 Budapest 112, Hungary; <sup>†</sup>Research Institute for Solid State Physics and Optics, Hungarian Academy of Sciences, P.O. Box 49, 1525 Budapest 114, Hungary; and <sup>‡</sup>Research Laboratory of Materials and Environmental Chemistry, Chemical Research Center, Hungarian Academy of Sciences, P.O. Box 17, 1525 Budapest, Hungary

Received April 30, 2001; accepted August 2, 2001

**Detailed thermoanalytical experiments were carried out to reveal the oxidative and reductive processes in the  $\text{Bi}_2\text{TeO}_5/\text{Bi}_2\text{TeO}_6$  system. The oxidation of  $\text{Bi}_2\text{TeO}_5$  starts at about 450°C but completed oxidation can only be achieved in oxygen ambient with a 670°C isothermal treatment. The decomposition of  $\text{Bi}_2\text{TeO}_6$  starts at 663°C. Above 790°C the loss of  $\text{TeO}_2$  is evident. The oxidation rate of  $\text{Bi}_2\text{TeO}_5$  single crystals is extremely low and develops a very complicated reaction interface changing in the course of reaction.** © 2001 Academic Press

**Key Words:** bismuth tellurite;  $\text{Bi}_2\text{TeO}_5$ ; oxidation; TG; DSC; TG-MS; optical materials.

### INTRODUCTION

Bismuth tellurite,  $\text{Bi}_2\text{TeO}_5$ , is a nonlinear optical material with interesting properties. Its crystals exhibit a long-living photorefractive signal that develops in the four-wave mixing experiments without any fixing process and lasts for years in the dark (1, 2). Homogeneous and high-quality  $\text{Bi}_2\text{TeO}_5$  single crystals can be grown from the melt by the Czochralski technique (3). Experimental investigations of the crystals have revealed anomalies in the physical properties of the material.

The crystal structure of the bismuth tellurite,  $\text{Bi}_2\text{TeO}_5$ , can be described as a  $2 \times 3 \times 1$  multiplication of a perturbed  $\text{CaF}_2$  type cell. The required cation charge is  $4+$  in this lattice, and the missing positive charge of the  $\text{Bi}^{3+}$  ions is compensated by a large number (17%) of empty oxygen positions (4).

The oxidation state is an important question in the  $\text{TeO}_2$ -based binary oxides. In these compounds the Te has  $4+$  charge at room temperature as well as at the melting point. Between these temperatures, however,

there is a region where the  $\text{Te}^{6+}$  is the stable charge. For the 1:1  $\text{Bi}_2\text{O}_3\text{--TeO}_2$  system, the fully oxidized  $\text{Bi}_2\text{TeO}_6$  composition is thermodynamically stable between 550°C and 700°C. Consequently, the cooling of the  $\text{Bi}_2\text{TeO}_5$  crystals grown from the melt includes a temperature range where oxidation and respective composition and structural changes may happen before room temperature is reached, deteriorating the quality of the single crystals.

Though the improper oxygen content plays an important role in the physical properties of the actual samples, only a few papers deal with the oxidation of the  $\text{Bi}_2\text{TeO}_5$ . Frit and Jaymes were the first, who studied the oxidation of  $\text{Bi}_2\text{TeO}_5$  and determined the crystal structure of  $\text{Bi}_2\text{TeO}_6$  by X-ray diffraction (5). Accordingly, the oxidation does not simply fill the empty oxygen positions, but it results in structural changes in the unit cell. They found that the oxidation starts at 400–500°C and the  $\text{Bi}_2\text{TeO}_6$  composition is stable up to 730°C. Gospodinov and Gjurova concluded that the oxidation of  $\text{Bi}_2\text{TeO}_5$  begins at 450–500°C and is completed around 600°C. The decomposition of the bismuth tellurate begins at about 700°C (6).

The actual excess oxygen residue in the room temperature  $\text{Bi}_2\text{TeO}_5$  crystals can be characterized by Raman spectroscopy (7). The intensity of a specific Raman line at  $762\text{ cm}^{-1}$ , with the incident and emitted line directions of  $[010]$  and  $[100]$  and incident and emitted light polarizations of  $[100]$  and  $[001]$ , respectively, was shown to be sensitive to the oxidation status of  $\text{Bi}_2\text{TeO}_5$  crystals. Accordingly, in the good-quality  $\text{Bi}_2\text{TeO}_5$  crystals the amount of the excess oxygen was detectable but not remarkable. The bulk oxidation of the crystals was not efficient under 550°C.

The aim of the present paper is the detailed study of the  $\text{Bi}_2\text{TeO}_5 + \text{O}_2 \rightarrow \text{Bi}_2\text{TeO}_6$  oxidation and the  $\text{Bi}_2\text{TeO}_6 \rightarrow \text{Bi}_2\text{TeO}_5 + \text{O}_2$  decomposition reactions.

<sup>1</sup>To whom correspondence should be addressed. E-mail: poppl@para.chem.elte.hu.



## EXPERIMENTAL

**Samples.** Most of the experiments were carried out on powder samples. Pieces of  $\text{Bi}_2\text{TeO}_5$  single crystal grown in air by the Czochralski technique from a Pt crucible (3) were ground in an agate mortar and sieved. The fraction with a grain size smaller than  $63\ \mu\text{m}$  was used for the investigations.

For microscopic investigations prismatic samples with dimensions of  $8 \times 5 \times 2\ \text{mm}^3$  were prepared from the bulk crystals by cleaving along the (100) plane, cutting and polishing along the (001) and (010) planes.

**Equipment.** The thermogravimetric (TG) experiments were carried out by using a Mettler TA-1 thermoanalyzer equipped for computerized data acquisition. One charge of the samples was about 100 mg, measured in an alumina crucible of 5 mm height and 8 mm diameter. The powdered samples were compacted by 30-s vibrations before the experiments. The thermobalance was evacuated to 0.1 mbar before each run and filled with the appropriate gas. Air, pure oxygen, argon, and different argon + oxygen mixtures were used at a flow rate of  $\sim 75\ \text{cm}^3/\text{min}$ . The measured TG curves were corrected for the buoyancy effect by measuring 100 mg of powdered aluminum oxide under the same experimental conditions. The DTG curves were obtained by a spline smoothing procedure. Heating and cooling rates were varied between 1 and  $10^\circ\text{C}/\text{min}$  and isothermal sections at various temperatures were also employed. The single crystals studied by thermogravimetry

were subjected to prolonged isothermal section. They were heated to  $670^\circ\text{C}$  at  $4^\circ\text{C}/\text{min}$ , and kept isothermally for 51.5 h.

The thermal decomposition of  $\text{Bi}_2\text{TeO}_6$  was studied by coupling a Balzers QMS 420 quadrupole mass spectrometer to the thermoanalyzer via a GES10 capillary inlet interface heated to about  $120^\circ\text{C}$  (TG-MS). The working gas was 6 N helium at a flow rate of  $85\ \text{cm}^3/\text{min}$ . Mass spectral scans were made continuously at a scan rate of 100 ms/amu and the electron impact (EI) mass spectra obtained at 70 eV were recorded.

The  $\text{Bi}_2\text{TeO}_6$  samples were prepared inside the thermoanalyzer equipment.  $\text{Bi}_2\text{TeO}_5$  powder was heated in oxygen ambient at a  $4^\circ\text{C}/\text{min}$  heating rate to  $670^\circ\text{C}$ , followed by a 180-min isothermal section.

The DSC measurements were carried out by using a PL Thermal Sciences 1500 differential scanning calorimeter (DSC) equipped with a data acquisition and evaluation system, in a flowing oxygen and argon atmosphere ( $10\ \text{cm}^3/\text{min}$ ), using  $4^\circ\text{C}/\text{min}$  heating rates. The sample weight was  $\sim 50\ \text{mg}$ , and the crucible material was platinum. The temperature and heat flow response of the calorimeter were calibrated using 6 N purity metals.

## RESULTS

### Examinations in Air Atmosphere

The most characteristic features of the  $\text{Bi}_2\text{TeO}_5 + 1/2\text{O}_2 \rightleftharpoons \text{Bi}_2\text{TeO}_6$  reaction in air atmosphere can be seen in Fig. 1. During heating in air flow the oxidation becomes

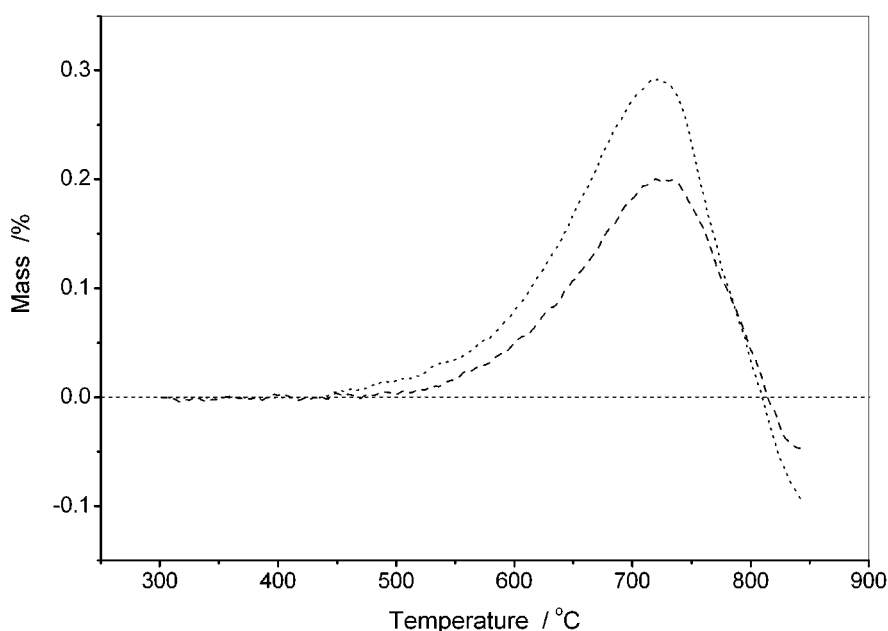


**FIG. 1.** The change of the sample mass during the thermogravimetric experiments of  $\text{Bi}_2\text{TeO}_5$  in air atmosphere at  $2^\circ\text{C}/\text{min}$  (····) and  $4^\circ\text{C}/\text{min}$  (---) heating rates.

observable around 450°C. The reaction rate is low and it depends strongly on the heating rate. The lower the heating rate, the higher the mass gain. Above ~ 730°C the decomposition reaction dominates and a mass loss can be observed. Note that the mass decreases below the initial sample mass above 800°C.

The theoretical mass gain for the oxidation reaction is 2.56%. In air flow, however, only 0.2–0.3% mass gain was observed, even at the low heating rate, 2°C/min. For this reason, further experiments have been carried out in a pure oxygen atmosphere.

### *The Main Features of the Reaction in the Oxygen Atmosphere*

Figures 2a and 2b show the thermogravimetric and DSC curves, respectively, at 4°C/min heating and cooling rate. During the heating, the oxidation starts at 456°C and the maximum reaction rate is reached at 674°C. The oxidation process is strongly exothermic. Above 761°C the decomposition of Bi<sub>2</sub>TeO<sub>6</sub> dominates, which is an endothermic process. The exothermic oxidation and the endothermic decomposition overlap each other at the

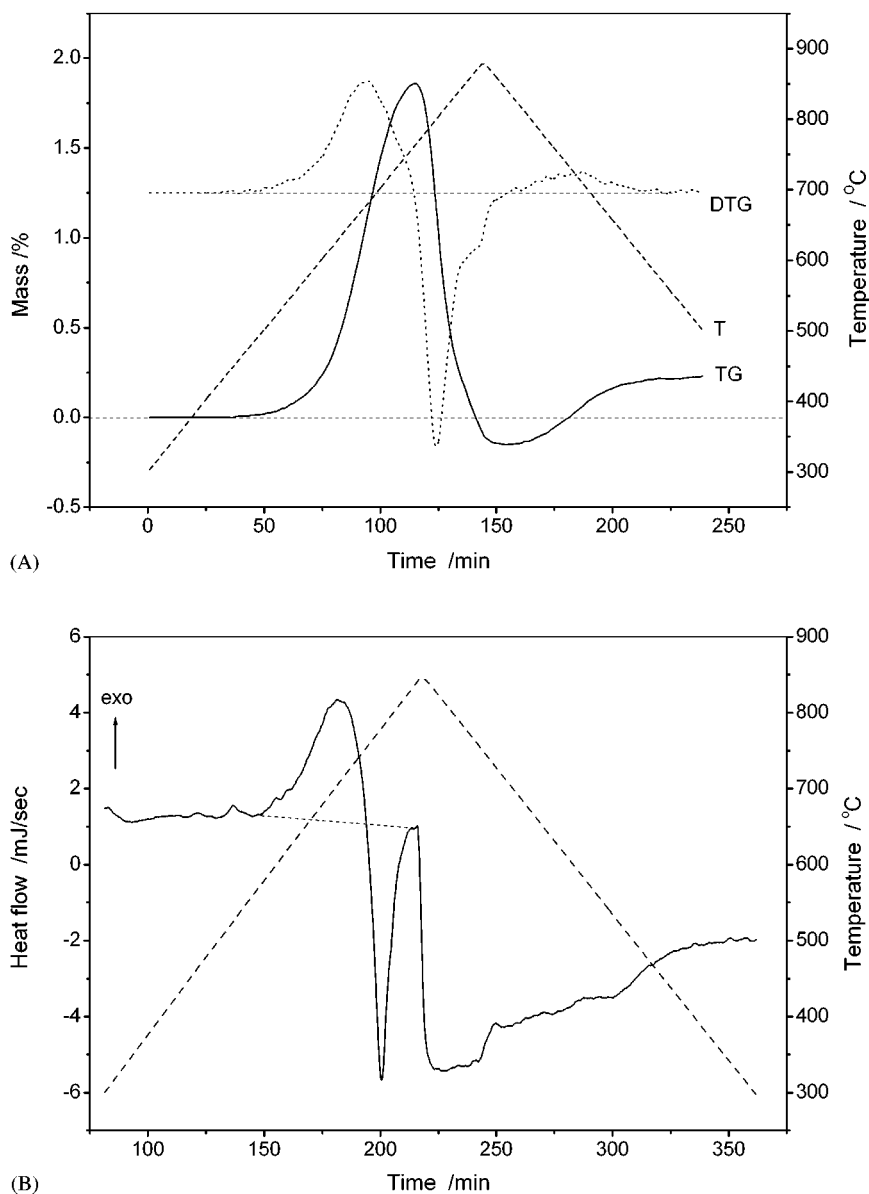


**FIG. 2.** Investigation of the oxidation and decomposition reactions by TG (A) and DSC (B) applying 4°C/min heating and cooling rates in oxygen ambient. In (B) an approximate baseline (---) was drawn to the DSC curve (—) in the heating section to indicate the magnitude of the exothermic and endothermic effects.

**TABLE 1**  
**Mass and Heat Changes during Heating and Cooling of Bi<sub>2</sub>TeO<sub>5</sub> at 4°C/min in Oxygen and Argon Atmosphere**

Ambient	Program	Temp range (°C)	Mass change (%)	DTG <sub>peak</sub> (°C)	ΔH (mJ/mg)
O <sub>2</sub>	Heating	456–761	+ 1.86	674	– 87
	Heating	761–835	– 2.01	798	59
	Cooling	845–578	+ 0.37	710	—
Argon	Heating	790–890	– 0.12	—	—

heating rate used, and reliable enthalpy changes could not be determined.

The thermoanalytical results at 4°C/min are summarized in Table 1. The data show that the measured mass gains with the 4°C/min heating rate are still smaller than the expected 2.56% value for the stoichiometric Bi<sub>2</sub>TeO<sub>6</sub> production. The incomplete oxidation is due to the decomposition of the formed Bi<sub>2</sub>TeO<sub>6</sub> at higher temperatures before the oxidation is finished. When the Bi<sub>2</sub>TeO<sub>6</sub> decomposes at higher temperature, a larger mass loss was observed than the mass gain during the oxidation. The difference may be explained by assuming the sublimation of TeO<sub>2</sub>. To check this assumption, a Bi<sub>2</sub>TeO<sub>5</sub> sample was heated in an argon atmosphere to 890°C at a rate of 4°C/min, and a mass loss of 0.12% was observed between 790°C and 890°C. This amount corresponds to the difference between the measured mass gain and mass loss within the experimental error (Table 1).

During the cooling period, the Bi<sub>2</sub>TeO<sub>5</sub> starts to oxidize again at 845°C, as indicated by mass gain in the TG experiments (Fig. 2a) and the baseline shift of the DSC experiments in the exothermic direction (Fig. 2b). The mass of the sample is practically constant below 500°C and the oxidized form is stable even at room temperature for a long period.

It is worth mentioning that much less oxidation occurs in the cooling section than in the heating section. The corresponding mass gain is about one-fourth of the value measured during the heating. The explanation of this observation requires further investigations. We plan to return to this question in a later paper.

#### Detailed Investigation of the Oxidation Process

Figure 3a compares the experiments with 670°C isothermal section. The TG curves indicate that the oxidation reaction was not far from completion in the reaction times employed. The reaction rate is acceleratory in the heating section and decelerating in the isothermal section. Note that a greater part of the reaction occurs in the isothermal section at the highest heating rate, 10°C/min, since the fraction reacted during the heating to 670°C was only 0.18 in that case. At low heating rates 1, 2, and 4°C/min the

reaction started at 456°C. At 10°C/min, the start of the reaction shifted to 480°C.

Figures 3b and 3c demonstrate the dependence of the reaction rate on the isotherm temperature and on the partial pressure of oxygen, respectively. Increasing the temperature above 670°C, the rate decreases and the completion of the reaction needs a longer time.

#### The Thermal Stability of Bismuth Tellurate

According to the previous section, perfect oxidation of Bi<sub>2</sub>TeO<sub>5</sub> (more than 2.5% mass gain) can be achieved by keeping the powdered sample at 670°C for 2–4 h. The thermal properties of the prepared Bi<sub>2</sub>TeO<sub>6</sub> are shown in Fig. 4 and Table 2. Heating in Ar ambient with a 4°C/min heating rate, Bi<sub>2</sub>TeO<sub>6</sub> is stable up to 663°C. The decomposition has a maximum velocity at 789°C and the process is completed by 860°C. The gaseous reaction products consisted entirely of oxygen ( $m/z = 32$  and 16). The measured mass loss is close to the theoretical value within the experimental uncertainty. Note that the mass spectrometer cannot detect sublimation species (TeO<sub>2</sub> and/or Te) since the connection between the MS and the TG and inlet system cannot be heated to properly high temperatures.

#### Study of the Oxidation on a Single Crystal

The results outlined in the previous sections suggest that the diffusion of the oxygen has an important effect on the reaction rate. To get a better insight into the factors influencing the diffusion, the reaction was also carried out on a single crystal. The crystal has a prismatic shape with a surface area of 212 mm<sup>2</sup>. In that case, the reaction rate was very slow; 51.5 hours were needed to achieve a mass gain of 0.6% (Fig. 5). The shape of the curve is particularly interesting. Though the reaction becomes observable below 670°C, it was so slow that the mass gain could be neglected during the heating period. The reaction rate showed a deceleration in the first 500 min in the isothermal section (magnified part of Fig. 5). However, thereafter an acceleration of the reaction happened that lasted until the end of the experiment. The acceleration suggests the gradual increasing of the reaction surface due to the developing of internal channel structures during the experiment.

#### Microscopic Observations

Microscopic examinations often provide positive evidence for interpretation of shapes of thermoanalytical curves, especially when microscopic defect structures are formed during the thermal reactions. We studied the topochemistry existing in the course of the Bi<sub>2</sub>TeO<sub>5</sub> + O<sub>2</sub> reaction by optical microscopy, using reflected (Figs. 6a and 6b) and transmitted illumination (Figs. 6c, 6d, and 6e).

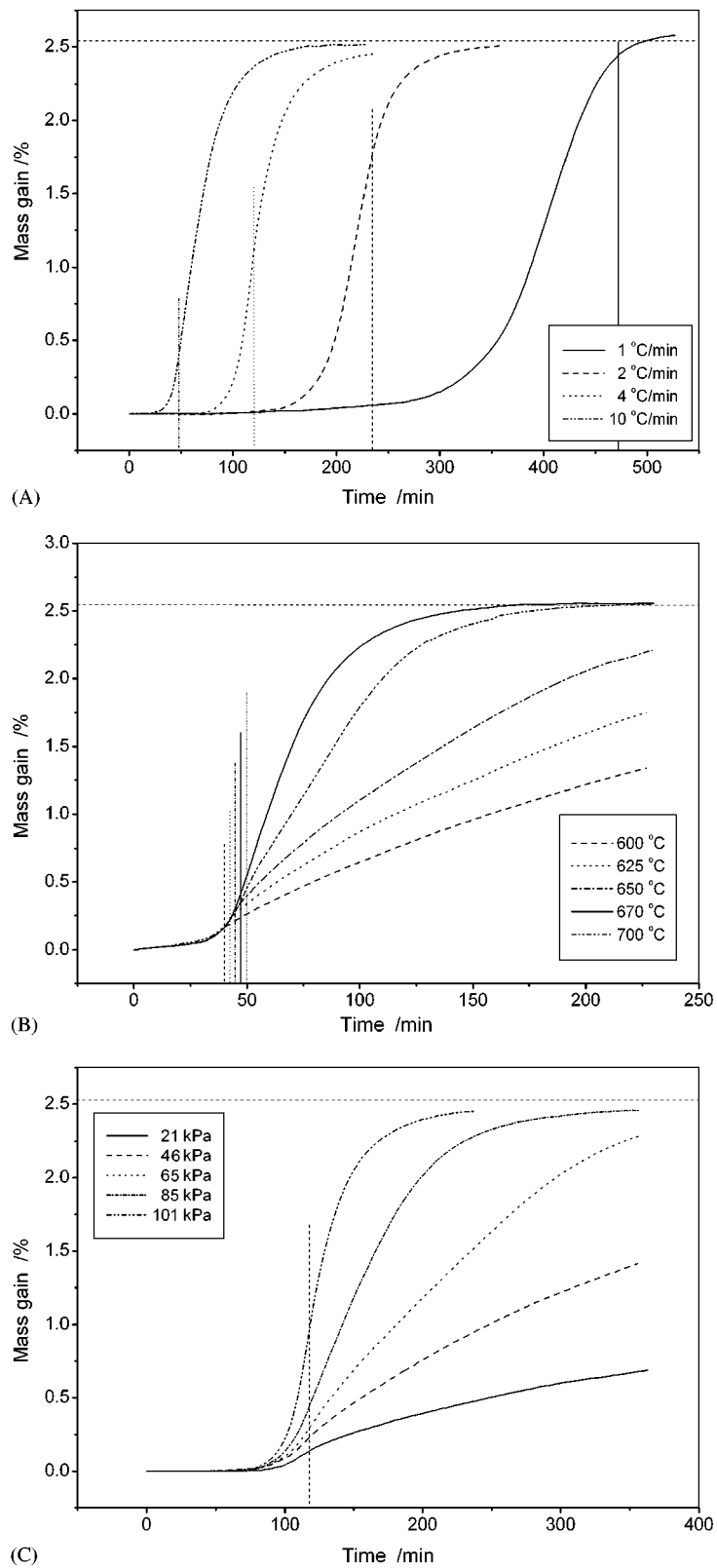


**FIG. 3.** Detailed thermogravimetric study of the oxidation of  $\text{Bi}_2\text{TeO}_5$ . The temperature program was complemented by an isothermal treatment in each case. The vertical lines represent the starting point of isothermal temperature. (A) Effect of different heating rates at a common isothermal temperature, 670°C. (B) Effect of different isothermal temperatures at a common heating rate, 4°C/min. (C) Effect of different oxygen concentrations in the ambient at a common temperature program (4°C/min and the subsequent isothermal annealing at 670°C).

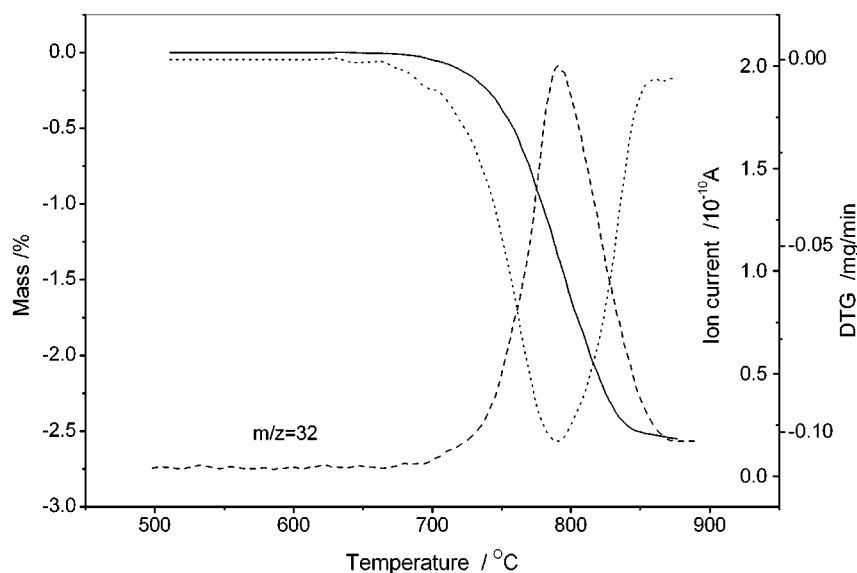


**FIG. 4.** Thermal decomposition of  $\text{Bi}_2\text{TeO}_6$  in He ambient, followed by a combined thermoanalytical and mass spectrometric method with  $4^\circ\text{C}/\text{min}$  heating rate. The mass spectrometric signal (---) shows the rate of the oxygen release.

The microscopic pictures have shown that the oxidation strongly depends on the crystallographic orientation of the open surfaces. Only the surfaces (001) and (010) were reacted fully, on which the microcrystalline structure of a product layer could be observed (Fig. 6a). The central part of the (100) plane shows a very complex morphological structure (Fig. 6b). It seems that the reaction starts at selective sites of the surface from which cracks and channels develop. It is revealed from the detailed examina-

tions that microcracks penetrate along the [041] direction, which is the oxygen plane in the  $\text{Bi}_2\text{TeO}_5$  structure. The other parts of the surface seem to be unreacted, but some dune-like features can be observed. This indicates that the reaction proceeds below the surface and the reactive volume becomes larger, probably due to the microcrystalline structure of the  $\text{Bi}_2\text{TeO}_6$  already produced. Investigating the crystal in the transmitted light all of these morphological characteristics can be observed. As the reaction proceeds

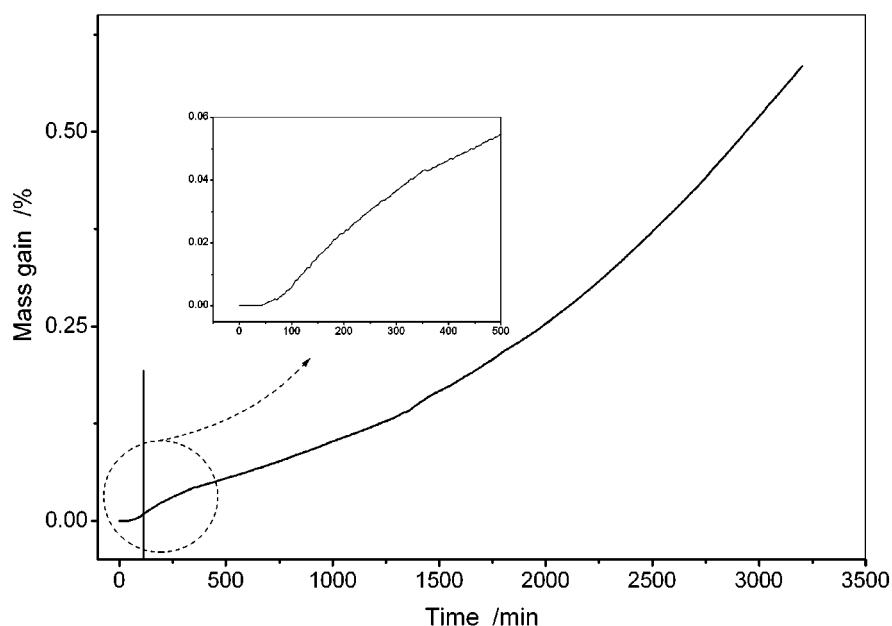


**FIG. 5.** Oxidation of a  $\text{Bi}_2\text{TeO}_5$  single-crystal sample in oxygen ambient. The heating period ( $4^\circ\text{C}/\text{min}$ ) was followed by an isothermal annealing at  $670^\circ\text{C}$  for 51.5 h.

**TABLE 2**  
**Decomposition of  $\text{Bi}_2\text{TeO}_6$  in Argon and Helium Atmosphere**

Ambient and heating rate	Temp range (°C)	Mass change (%)	DTG <sub>peak</sub> (°C)	$\Delta H$ (mJ/mg)
Argon, 4°C/min	663–860	– 2.53	789	190
Helium, 10°C/min	677–890	– 2.58	805	—

into the crystal, needle-like cracks and channels develop, which undergo branching and build up fan-shaped product morphology. This generates a very complicated reaction interface growing over the course of the reaction, which is the reason for the acceleratory region of the TG curve.

### CONCLUSIONS

The specific oxidative and reductive processes in the  $\text{Bi}_2\text{TeO}_5/\text{Bi}_2\text{TeO}_6$  system were studied by detailed ther-

moanalytical experiments. Using powdered  $\text{Bi}_2\text{TeO}_5$  samples, the oxidation starts at about 450°C but complete oxidation can be achieved only by long annealing of the samples in oxygen ambient at 670°C. At higher temperatures the  $\text{Bi}_2\text{TeO}_6$  decomposes. Above 790°C the loss of  $\text{TeO}_2$  is also evident. With the regular thermoanalytical heating rates (2–10°C/min) the oxidation and reduction sections overlap each other. Using combined mass spectrometric and thermoanalytical investigations it was shown that starting from pre-prepared  $\text{Bi}_2\text{TeO}_6$ , the decomposition begins at about 670°C and, losing oxygen, the  $\text{Bi}_2\text{TeO}_5$  composition is restored by 860°C.

The oxidation rate of  $\text{Bi}_2\text{TeO}_5$  single crystals is extremely low and the thermal treatment destroys only a thin surface layer of the samples. Thus, the oxidation and subsequent reduction do not influence the bulk quality of the single crystals grown from the melt and slowly cooled to room temperature during the growth.

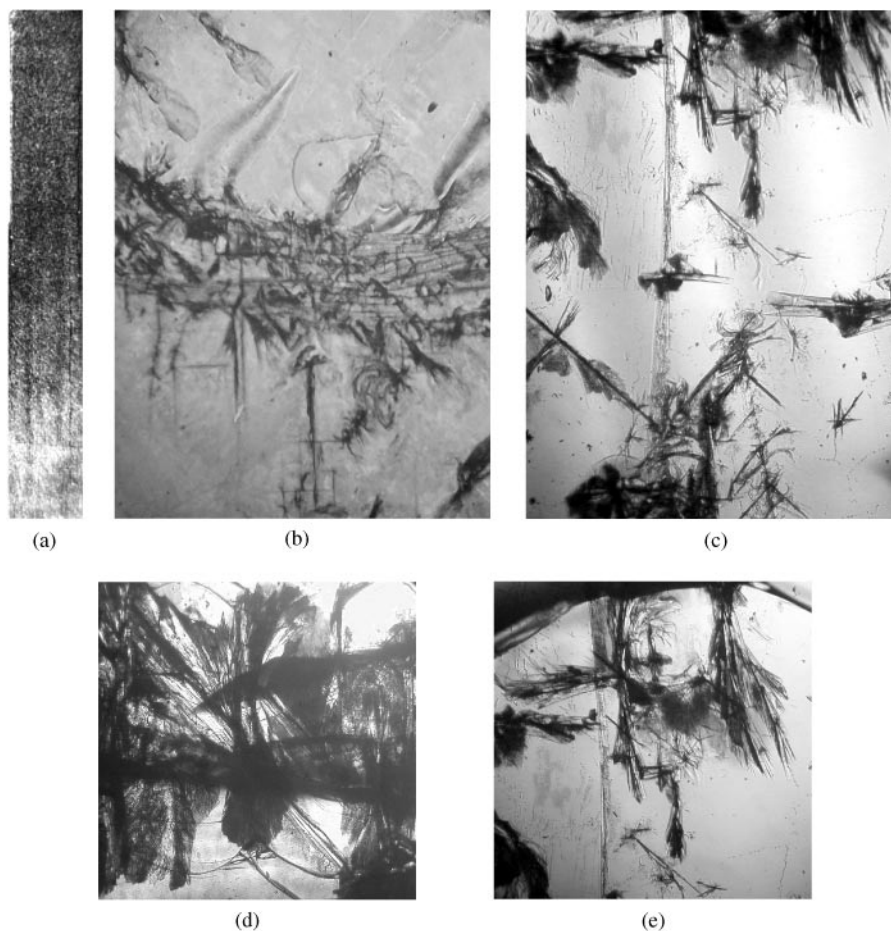


**FIG. 6.** Optical microscope pictures of the partly reacted ( $\alpha = 0.23$ )  $\text{Bi}_2\text{TeO}_5$  single crystal. (a) (010) Plane of the crystal covered by microcrystalline product layer. Magnification:  $20\times$ . (b) Selected part of the (100) plane illuminated by reflected light. The picture shows the complicated product structure consisting of cracks and channels. The sand-hill-like formations indicate that the reaction proceeds below the surface. Magnification:  $120\times$ . (c–e) Selected parts of the (100) plane illuminated by transmitted light. (Magnifications were  $63\times$  and  $120\times$  in d and e, respectively.) These pictures prove that the cracks and channels developed during the reaction penetrate into the reactant crystal and generate a very complicated reaction interface.

## ACKNOWLEDGMENTS

This work was supported by the Hungarian Research Found OTKA (Grants T 026647 and T 029756). The authors express their gratitude to Mrs. Á. Péter for helpful discussions, and to Mrs. I. Perzcel, Mr. G. Matók, and Mrs. A. Somló for their assistance in the crystal growth, crystal processing, and thermoanalytical measurements, respectively.

## REFERENCES

1. I. Földvári, H. Liu, R. C. Powell, and Á. Péter, *J. Appl. Phys.* **71**, 5465–5473 (1992).
2. Á. Péter, O. Szakács, I. Földvári, L. Bencs, and A. Munoz, *Mater. Res. Bull.* **31**, 1067–1073 (1996).
3. I. Földvári, Á. Péter, R. Voszka, and L. A. Kappers, *J. Crystal Growth* **100**, 75–77 (1990).
4. D. Mercurio, M. El Farissi, B. Frit, and P. Goursat, *Mater. Chem. Phys.* **9**, 467–476 (1983).
5. B. Frit and M. Jaymes, *Bull. Soc. Chim. Fr.* **78**, 402–406 (1974).
6. G. G. Gospodinov and K. M. Gjurova, *Thermochim. Acta* **83**, 243–252 (1985).
7. I. Földvári, R. S. Klein, G. E. Kugel, and Á. Péter, *Rad. Eff. Def. Solids* **151**, 145–149 (1999).